Available online at www.sciencedirect.com
SCIENCE DIRECT®
Journal of Nuclear Materials 335 (2004) 232–238
journal of nuclear materials
www.elsevier.com/locate/jnucmat

Preliminary results of post-irradiation examinations on LiSoR-2 test section

Y. Dai *, H. Glasbrenner, V. Boutellier, R. Bruetsch, X. Jia, F. Groeschel

Paul Scherrer Institut, 5232 Villigen PSI, Switzerland

Abstract

Liquid–solid reaction under irradiation (LiSoR) experiments are aimed at understanding the effects of liquid lead–bismuth eutectic (LBE) corrosion and embrittlement under irradiation on structural materials, which is one of the key items of the materials R&D for the future accelerator-driven system (ADS). The LiSoR setup is basically a LBE loop with a test section irradiated with 72 MeV protons. The second irradiation was conducted for about 34 h and terminated after a leakage of LBE was detected. Post-irradiation examinations (PIE) are being performed on both the tube and tensile specimen in the test section. Optical microscopy, scanning electron microscopy, transmission electron microscopy and microhardness tests have been completed. The results show that a crack formed in the irradiation zone of the tube. In the material in the irradiation zones of both the tube and the tensile specimen dislocation cell structure is well developed, which indicates heavy deformation due to thermal fatigue. The crack should start at the inner surface and propagate to the outer surface. The fracture surfaces of the crack are dominated by a brittle cleavage fracture mode. However, on the surfaces of the tensile specimen, no microcracks are observed.

1. Introduction

Liquid lead–bismuth eutectic (LBE) has been considered as both the coolant in the core and the target material in the spallation target of a future accelerator-driven system (ADS) for transmutation of nuclear waste [1,2]. One of critical issues for operating an ADS device is related to the structural materials used in the heavy irradiation areas such as the target and the core. The structural materials in the target, particularly those at the proton beam window, will be exposed to intensive irradiation in the presence of relatively high mechanical loads, while LBE corrosion and embrittlement effects cannot be excluded. To understand the behavior of the structural materials used in the target is of essential importance for a safe operation of the system.

For developing such an ADS device, an international project, MEGAPIE – 1 Megawatt Pilot Experiment, was launched to demonstrate the feasibility of operating a liquid metal target by using the existing spallation neutron facility (SINQ) at PSI [3,4]. In the MEGAPIE target, LBE will be used as the target material and martensitic steel T91, one of candidate structural materials for the ADS, will be used for the LBE container. Therefore, to the MEGAPIE project and also the materials technology of the ADS program, it is important to study the properties of T91 in an irradiation and LBE corrosion environment.

* Corresponding author. Tel.: +41 56 310 4171; fax: +41 56 310 4529.
E-mail address: yong.dai@psi.ch (Y. Dai).

0022-3115/$ - see front matter © 2004 Elsevier B.V. All rights reserved.
doi:10.1016/j.jnucmat.2004.07.026

LiSoR experiments were proposed for investigating the behavior of materials in liquid metals under the irradiation of 72 MeV protons produced by Injector-I at the Paul Scherrer Institut (PSI), Switzerland [5]. Preliminary neutronic calculations indicated that the irradiation of 72 MeV protons could closely simulate that of 600 MeV protons in terms of radiation damage rate, helium, hydrogen and other transmutation elements production. With collaboration between PSI and Subatech, France, a LBE loop has been set up [6]. The test section of the loop consists of a tube and a tensile specimen. The specimen is stressed in tension to a mechanical load of 200 MPa during irradiation to simulate the effects of the mechanical load and irradiation at the beam window of the MEGAPIE target. The second irradiation was conducted for about 34 h and terminated after a leakage was detected [7]. In this experiment, the irradiation zone of the tube in the test section was overheated due to wobbling beam at a too low of frequency. The material in the irradiated area was deformed by thermal fatigue. Finally a crack developed and resulted in the leakage. The post-irradiation examinations (PIE) are being performed on both the tube and tensile specimen. The present paper will show results of the visual inspections and scanning electron microscopy (SEM) and transmission electron microscopy (TEM) investigations.

2. Experimental

2.1. Material and specimens

The details of the LiSoR facility can be found in the previous report [6]. The parts exposed to the proton beam are the tube and tensile specimen in the test section. The test section has a length of about 140 mm. The shape of the tube and the dimensions of the cross-sections of the tube and the tensile specimen is illustrated in Fig. 1. Although the tube and the tensile specimen are both made of martensitic steel T91, the steels for the two parts are slightly different due to the different sources. The T91 steel used for the tube was purchased from Creusot Loire Industrie (France) and has a composition in wt% of 8.26Cr, 0.13Ni, 0.95Mo, 0.43Si, 0.38Mn, 0.1C, 0.2V, 0.017P, 0.065Nb, and with Fe in balance. While the T91 steel used for the tensile specimen was obtained from SPIRE program produced by Ugine (France) and has a composition in wt% of 8.63Cr, 0.23Ni, 0.95Mo, 0.31Si, 0.43Mn, 0.1C, 0.21V, 0.02P, 0.09Nb, and with Fe in balance. Both materials have the standard heat treatment, namely normalized at 1040 °C for 1 h followed by air cooling, and then tempered at 760 °C for 1 h followed by air cooling. The outer surfaces of the tube were milled and the inner surfaces were cut with an electron discharging machine (EDM). Both the outer and inner surfaces were irradiated without any further polishing. The tensile specimen was also cut by an electron discharging machine. Its surfaces were polished mechanically and finished with 1000 grit grinding papers.

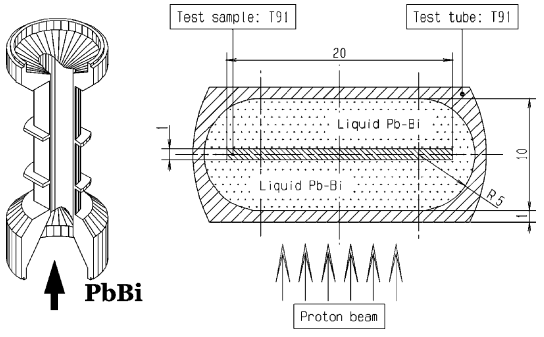

Fig. 1. Sketches showing the tube of the LiSoR test section and the cross-section of the tube including the test specimen. The dimensions are in millimeters.

Impag AG (Switzerland) supplied the eutectic Pb–55.5Bi (44.8 wt% Pb and 55.2 wt% Bi) alloy which contained as little as only a few ppm of impurities: Ag 11.4, Fe 0.78, Ni 0.42, Sn 13.3, Cd 2.89, Al 0.3, Cu 9.8, Zn 0.2.

In the LiSoR loop there is no possibility to measure or control the oxygen content due to the 'low' working temperature at which no oxygen sensor developed up to now gives reliable values. Anyway the filling of the loop is always performed with LBE melt having a temperature of around 250 °C whereas the oxygen content is very low due to the low solubility. This means that the oxygen content in the LBE at the operating temperature (300 °C) is below the oxygen saturation level (no formation of PbO which might block the pipes of the loop) but high enough to avoid dissolution of the steels iron oxides.

2.2. Irradiation of the LiSoR loop

The irradiation source is 72 MeV proton beam with a current of about 50 μA. In order to obtain a uniform irradiation zone, a small sized proton beam ($\sigma = 0.8$ mm) was wobbled over an area of about 14×5.5 mm^2 during irradiation. The wobbling had a frequency of 1.17 Hz in vertical and 14 Hz in horizontal directions.

Before the irradiation started, the temperature of LBE was about 250 °C. After the proton beam switched on, it increased to about 300 °C in the test section, which was measured at a position above the irradiation zone. However, there was no thermal couple directly attached on either the tube or the tensile specimen near or in the irradiated area. Therefore, the temperature of the tube and tensile specimen was not known during irradiation. Unfortunately, it was not carefully calculated before irradiation either. The results of the calculation done

after the irradiation using the ANSYS code are shown in Fig. 2(a) and (b) which indicate that: (1) the temperatures at difference positions are very different whereby the maximum temperature in each case is reached just after the turning point of the beam; (2) the temperature at one position oscillates at a frequency of 1.17 Hz; (3) the maximum temperature at the outer surface of the tube is about 780 °C, and the corresponding temperature at the inner surface is about 670 °C [7]. The temperature gradient of 110 °C cross the wall (1 mm thick) introduces a thermal stress of about 170 MPa, which is much higher than the yield stress of T91 at these temperatures. Therefore, the material in the irradiated zone of the tube should be subjected to thermal fatigue deformation during irradiation. For the tensile specimen, the temperature was lower due to cooling from both surfaces by flowing LBE. However, the heat deposition in the specimen was about 1.5 times of that in the wall of the tube [6]. This resulted in a maximum temperature at the middle of the specimen of about 620 and 580 °C at the surfaces. The 40 °C temperature difference across the 0.5 mm thickness gave a thermal stress of about 120 MPa. This thermal stress was in superposition with the stress of 200 MPa applied mechanically and resulted in also thermal fatigue deformation similar to that in the tube.

The irradiation lasted for 34 h and was terminated due to a detected leakage of LBE. The total proton charge of 1.6 mA h was received. The radiation damage produced in the irradiated zone is about 0.1 dpa (displacement per atom).

3. Results and discussion

3.1. Visual inspections

After dismounting the test section in a hot-cell, the tube and the tensile specimen were taken out. Photography was done and the four pictures in Fig. 3 illustrate the views of the front and back sides of the tube and the specimen. The photograph of the front side of the tube (Fig. 3(a)) shows clearly the proton beam footprint in the irradiation zone and also a crack existing in the irradiated zone. The black spot at the lower end of the crack is a heavy oxidized area rather than a hole (as it may appear). On the surfaces of the tensile specimen, the irradiation area can also be seen. While on the back side of the tube, no beam footprint can be seen. This indicates that the proton beam could not penetrate the

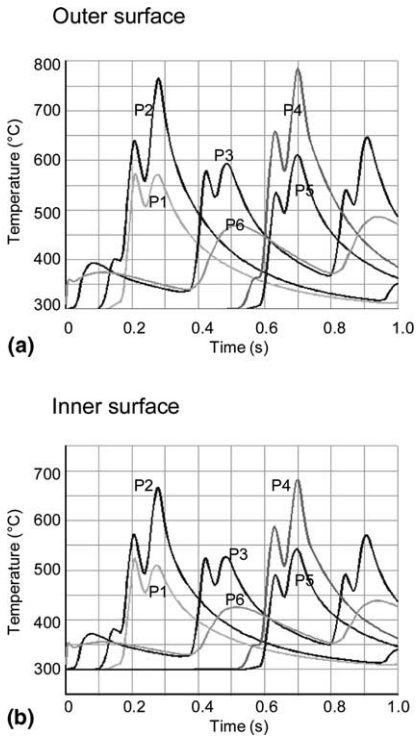

Fig. 2. Plots showing (a) outer and (b) inner surface temperatures at six positions in the irradiation zone of the tube.

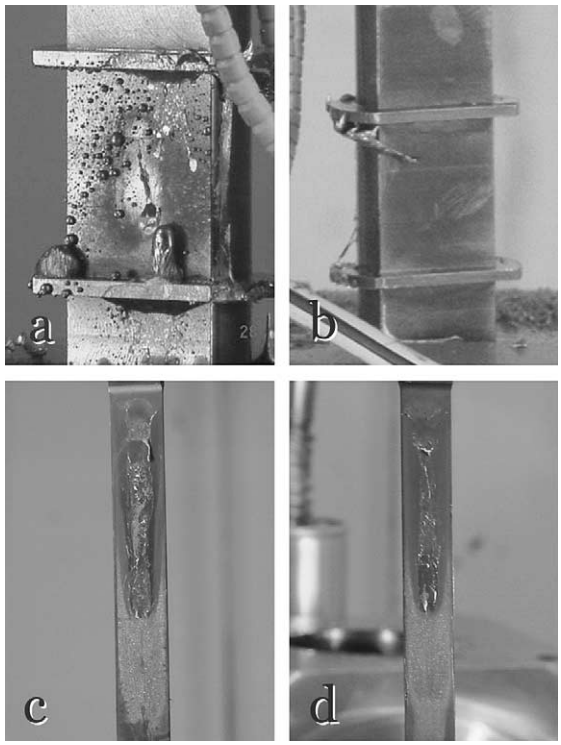

Fig. 3. Photographs showing the views of (a) the front side of the tube, (b) the back side of the tube, (c) the front side of the specimen and (d) the back side of the specimen.

whole test section which is in agreement with neutronics calculation [6].

On the surfaces of the specimen there is some Pb–Bi attached in the irradiation area and also in the region immediate above the irradiation area, where the temperature could be quite high due to the heat brought by the up-stream LBE. In the large region below the irradiation area, it looks like something deposited there.

3.2. SEM observations

Systematic SEM observation has been performed to study the LBE corrosion and irradiation effects on the tube and specimen.

3.2.1. The inner surface of the tube

Few samples were cut from the upper part of the tube where the material was not exposed to irradiation. Fig. 4(a) and (b) shows the views of the cross-section and inner surface away from the exposed region which was slightly polished for inspection, respectively. Micro-cracks of few tens microns long and up to ten microns deep were frequently observed. These microcracks were produced by EDM cutting rather than LBE corrosion or embrittlement. Under tension stress, such microcracks can propagate and become large cracks as observed in the irradiated area of the tube.

3.2.2. The crack in the irradiated zone of the tube

One of the main objectives of this study is to investigate the characteristics of the crack in the irradiated zone of the tube and find out where the crack initialized and how it propagated. The general feature of the crack can be characterized as brittle and ductile mixed fracture. Most of areas, particularly the central part, show brittle fracture (Fig. 5(a)). Only a small part near the outer surface and close to the upper end of the crack presents a typical ductile fracture mode (Fig. 5(b) lower part). This may indicate that the crack started at the inner surface and propagated to the outer surface. In the central part, the crack growth could be promoted by irradiation and LBE embrittlement effects, which

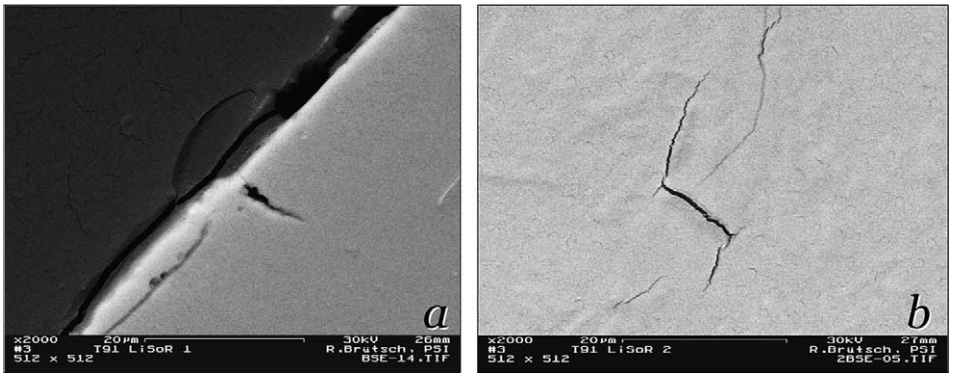

Fig. 4. Microcracks observed (a) at the cross-section and (b) on the inner surface at the upper part of the tube which was slightly polished for inspection.

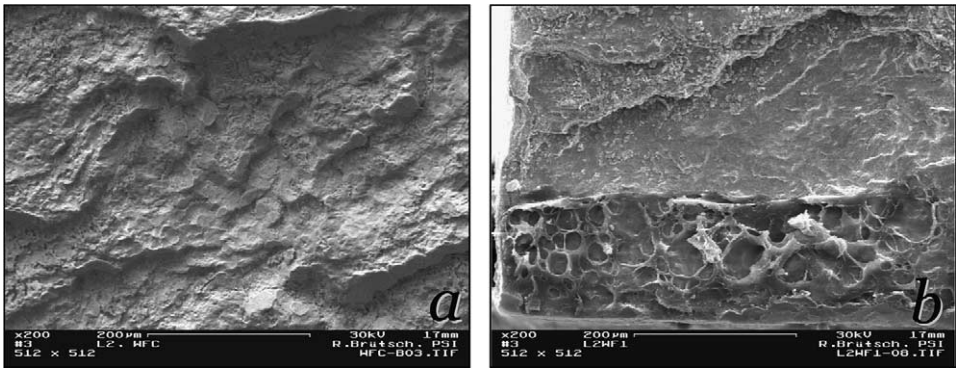

Fig. 5. Micrographs showing (a) brittle fracture in the central part and (b) ductile fracture in an area near the outer surface and close to the upper end of the crack.

resulted in a brittle fracture. The ductile fracture part at the upper end of the crack is less than 200 μm thick and could be broken at a relative high speed like tearing. The crack starting at the inner surface of the tube is understandable because microcracks in the surface layer were ready to propagate under high tension stress induced by the temperature gradient.

Since the inner surface was heavily oxidized by EDM cutting and also very rough, corrosion traces are not evident. While on the fracture surface there is a heavily corroded area at the lower part of the crack as can be seen in Fig. 6. The position of this area corresponds to that black spot at lower end of the crack seen in Fig. 3(a). The black spot or heavily oxidized area on the outer surface should indicate the area was once exposed to much higher temperature than the rest. This could happen when LBE seeped out through the crack, it might form drops at the lower crack end. A drop of LBE of 1–2 mm large would increase the temperature inside the wall easily to above 1000 °C. At such a high temperature, corrosion effects would be significant even in a short time period of 2 h, which is the time from the leak started until the irradiation was stopped. The shape of the area under the dash line reflects also the effects of the temperature gradient.

3.2.3. The surface of the tensile specimen

As mentioned above, 200 MPa tensile stress was applied to the tensile specimen and, meanwhile, in the irradiation zone a thermal stress of about 120 MPa was induced by the temperature gradient during irradiation. Under such a severe condition of high temperature, high stress and intensive irradiation, irradiation-assisted-

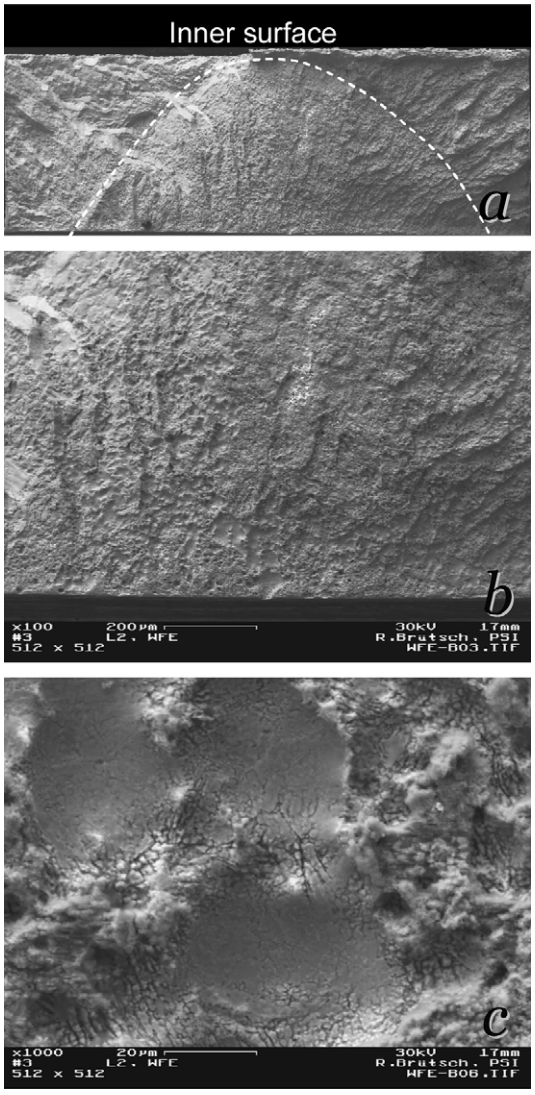

Fig. 6. Micrographs showing LBE corrosion in an area on the fracture surface at the lower part of the crack. (a)–(c) show the view at different magnifications.

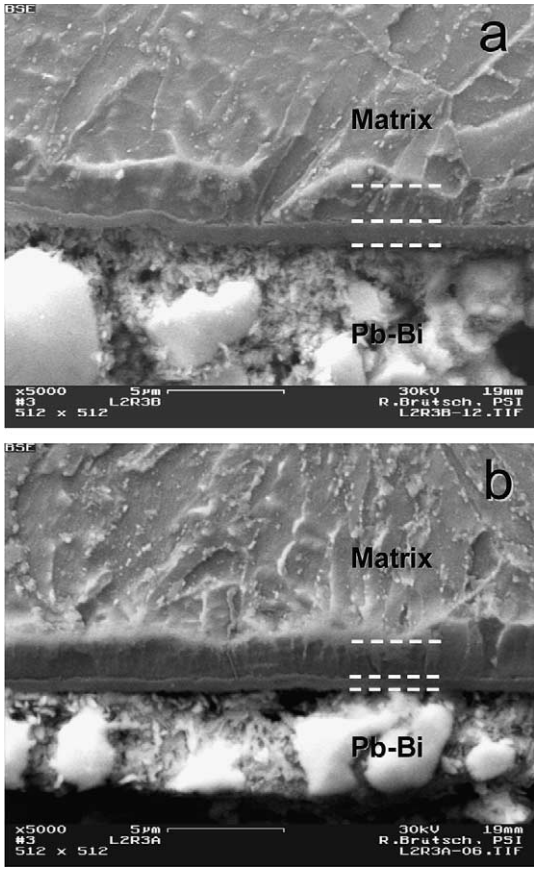

Fig. 7. Cross-sections of the tensile specimen: (a) perpendicular and (b) parallel to the tensile axis.

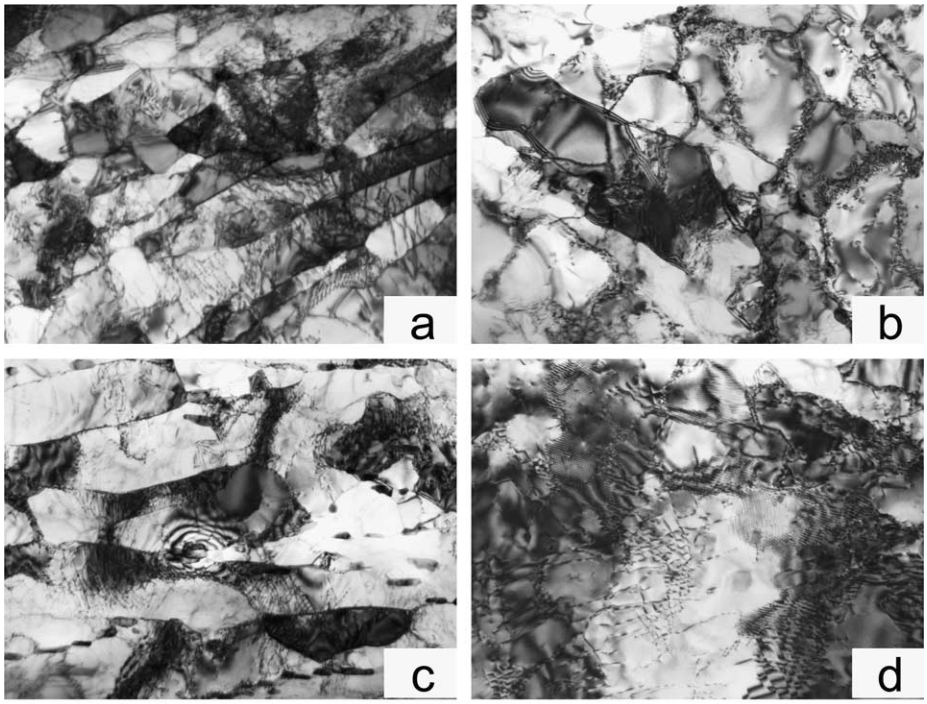

Fig. 8. Microstructure in material at positions: (a) above the irradiated area of the tube, (b) in the irradiated area of the tube, (c) below the irradiated area of the tensile specimen and (d) in the irradiated area of the tensile specimen. The scale represents 600 nm for (a), (b) and (c), but 400 nm for (d).

stress-corrosion-cracking (IASCC) is very likely to occur. However, on the cross-sections in both directions perpendicular and parallel to the tensile axis, there were no microcracks observed, as illustrated in Fig. 7. Instead of microcracks, a thin oxide layer formed on the surface. The oxide layer up to 3 μm thick was revealed only in the irradiated area. Outside the irradiated area no oxide layer was observed. In the oxide layer, two layers can be distinguished, which should be of the magnetite (outer layer) and spinel (inner layer) structure. The formation of the oxide layer is believed to be due to the high temperature experienced during irradiation.

3.3. Microstructural investigation

TEM observations have been carried out to investigate changes in the microstructure of the material after irradiation. Samples from four locations: in and above the irradiated area of the tube, in and below the irradiated area of the tensile specimen were examined. The microstructure at these four locations is presented in Fig. 8. Fig. 8(a) and (c) illustrates similar features of martensite lath structure in the original materials. While Fig. 8(b) shows that a subgrain structure has been well developed from dislocation cells, which indicates heavy deformation of the material. Fig. 8(d) demonstrates dislocation cells formed already and subgrains were being evolved, which means that the material is also deformed.

These results give a clear explanation to the failure of the tube: high thermal stress caused by the high temperature gradient across the wall introduced significant thermal fatigue. After about 100 000 cycles, hence followed by the wobbling frequency of the beam (the leakage started at around 32 h), the crack propagated through the wall and resulted in the leakage. On the other hand, it is interesting to note that there are no microcracks observed in the irradiated area of the tensile specimen, although the material was heavily deformed by thermal fatigue. The reason could be that the total deformation was still not high enough. However, it is believed that the smooth surfaces should be also a beneficial factor. The failure in the tube should be, at least, partially attributed the existing surface microcracks, which were ready to grow under such a stress level.

4. Conclusions

Post-irradiation examinations have been performed on the second LiSoR test section after a total irradiated

period of about 34 h. Following results have been obtained.

(1) The LBE leakage was due to a crack formed in the irradiation zone of the tube. The crack should be mainly attributed to thermal fatigue induced by high thermal stress and partially due to surface micro-cracks. The crack should start at the inner surface and propagate to the outer surface.
(2) The fracture surfaces of the crack are dominated with brittle fracture features, which may be assisted by LBE embrittlement effects. There are no micro-cracks observed on the surfaces of the tensile specimen.
(3) TEM observations demonstrate that the material in the irradiation zones of both the tube and the tensile specimen was deformed, while the material (as well tube and specimen) outside the irradiation zones was not deformed.

Acknowledgments

The authors would like to thank H.P. Linder, H. Schweikert, R. Thermer and D. Viol for their help on gamma measurements and sample preparation. This work is included in TECLA subprogram of the European 5th Framework Program and supported by the Swiss Bundesamt für Bildung und Wissenschaft.

References

[1] C. Rubbia, J.A. Rubio, S. Buono, F. Carmianti, N. Fietier, J. Galvez, C. Geles, Y. Kadi, R. Klapish, P. Mandrillioni, J.P. Revol, C. Roche, European Organisation for Nuclear Research, CERN report AT/95-44 (ET), 1995.
[2] L. Cinotti, M. Bruzzone, S. Cardini, G. Corsini, G. Saccardi, Doc. ANSALDO ADSI, SIFX 0500, June 2001.
[3] G.S. Bauer, M. Salvatores, G. Heusener, J. Nucl. Mater. 296 (2001) 17.
[4] F. Groeschel, these proceedings.
[5] Y. Dai, G.S. Bauer, Research proposal; Irradiation effects on the liquid metal embrittlement in structural materials for liquid metal target of spallation neutron sources, PSI, November 1997.
[6] T.T. Kirchner, Y. Bortoli, A. Cadiou, Y. Foucher, J.S. Stuzmann, T. Auger, Y. Dai, S. Dementjev, K. Geissmann, H. Glasbrenner, F. Groeschel, F. Heinrich, K. Kohlik, G. von Holzen, Ch. Perret, D. Viol, J. Nucl. Mater. 318 (2003) 70.
[7] H. Glasbrenner, Y. Dai, S. Dementjev, F. Gröschel, L. Ni, D. Viol, T. Kirchner, Technical Report, PSI, TM-34-02-04, November 2002.